The Optimization Model of Composite Material UAV Shooting Flight Routes

Ting Zheng*

College of Computer and Information, Inner Mongolia Medical University, Huhhot, Inner Mongolia, 010110, China

Abstract

UAV is one of the important achievements of scientific and technological innovation, which has been widely used in various fields of life in recent years. UAVs of composite materials are the most popular because the composite itself has designability, and can be optimized according to the strength and stiffness of the aircraft without changing the structural weight. In order to ensure the UAV to carry out more accurate image acquisition under the actual ground conditions, through the analysis of decision variables, this paper uses the linear weighting of image shooting range and pixel accuracy to establish the objective function, and establishes the optimal shooting angle under different constraints Considering the actual motion characteristics of objects such as automobiles, this paper assumes that the tracked ground targets are a class of motion objects with non-integrity constraints when the flight altitude of UAV is fixed and the flight speed is constant. The ground target model and the flight dynamics nonlinear model are established. This paper presents a new RRT* algorithm for path planning based on the obstacles encountered by UAV during flight, that is, using the cost function to select the node with the minimum cost in the field of expanding nodes as the parent node, using the MATLAB to select a reasonable obstacle avoidance strategy, the global optimal route is obtained by smoothing processing, and the data simulation test is carried out. The experimental results show that the model is robust.

Keywords: Composite Material UAV, Optical imaging, Golden section algorithm, Target tracking, RRT

I. Introduction

With the rapid development of technology, aerial photography of drones has entered people's work and life, including environmental monitoring [1,2], attacks [3], Search and rescue [4-6], and so on. That is, taking a picture of the earth from the air and obtaining a top view. It provides a new vision and more possibilities for shooting angle and direction, greatly enriching the content and picture under the previous shooting restrictions, and enhancing the layering and three-dimensionality of the work.

Today, aerial photography has provided important clues for film and television shooting, ecological protection, and big data. It is one of the important achievements of technological innovation since the 20th century. It is not only small in size, light in weight, low in noise, but also can replace humans in shooting high-definition aerial images. Therefore, the aerial photography technology of drones is an important product of the development of the times. In the aerial photography process, how to optimize the flight distance and shooting quality has become an important topic of discussion at home and abroad.

Gesang Nugroho described the manufacturing process of lightweight and strong UAV and composite aircraft flight testing capability [7], Victor San Juan and Matilde Santos proposed several methods to calculate the UAV discrete path planning [8], four methods are applied to calculate the path planning: an original proposal called attraction, fuzzy logic, ANFIS, and a PSO algorithm. Rodzewicz described of a novel approach to the load spectra estimation applied to UAVs. It is developed a number of tools in the LabVIEW environment enabling an in-depth analysis of flight-log data [9]. Goerzen provided an overview of existing motion planning algorithms while adding perspectives and practical examples from UAV guidance approaches [10]. Luitpold Babel introduced a new approach for three-dimensional flight path optimization for unmanned aerial vehicles [11]. many researchers have been looking into the problem of cooperative path-planning of multiple UAVs [12–14]. The more research on drones can be found in [15-20] references.

In order to solve the problem of low accuracy of shooting results, Huang Wei proposed a key target point spacing measurement based on aerial image of drone [21] .Zhou Xiaoli proposed that when the plane turns to the slope [22], the camera will be shot in an instant, so that the scene will form a slope line in the light and shadow, resulting in a sense of movement. Ji Yuan and others analyzed the main technical indicators [23] in photogrammetry operations, such as flying height and flight speed relative to the ground. Cheng Hao, Cao Jie et al. proposed a dual-image stereo positioning method based on drone for the problem that the target area of the UAV target area is not obvious and affects the target location [24]. In order to achieve target positioning.

For the first drone operator, it is difficult to master the techniques of flight altitude, flight speed and shooting angle. The flying height of the drone is too high or too low, which affects the size of the range collected by the camera and the number of pixels per unit area. The flight speed of the drone is inversely proportional to the number of frames taken per unit time by the camera.

Therefore, the main task of this paper is to analyze how to adjust the flying height, flight speed and shooting angle of the drone, and use the drone to take satisfactory photos, mainly complete the following four questions.

Task1: The drone performs aerial photography on a certain area in a straight flight mode. It is assumed that the drone is not affected by external factors such as wind direction, humidity, etc. during flight, and the flying height range of the drone, and best aerial photographing height at the specified shooting angle.

UAV technical parameters are analyzed in this paper, from the UAV itself and shooting pictures. The drone's own parameters include the flying height h, the flying speed v and the shooting angle θ. The parameters of the captured picture include the camera acquisition range area S, the pixel number DPI of the image per inch length, and the frame number P of the camera acquisition image per second. Then according to the topic, the image captured by UAV is the best. The objective function is established by linear weighting of the range and pixel accuracy of the image The optimal aerial height model for linear is established based on the flying height, pixel precision, flight speed and shooting angle.

Task2: The drone needs to perform more accurate image acquisition under actual ground conditions to solve the optimal range of UAV shooting angles. Among them, it is assumed that the flying height of the drone is fixed and the flying speed is constant.

Firstly, the decision variables are analyzed, including the shooting area and shooting angle, shooting area and pixel accuracy, flying height and shooting area, shooting angle and pixel accuracy. The improvement is then based on the optimal aerial height model for linear flight mode of task 1. The UAV shooting angle optimization model with the aim of shooting area and pixel precision, flying height, pixel precision, flight speed, pixel precision and camera acquisition range area is established.

Task 3: Assume that the drone's flight altitude is fixed and the flight speed is constant, and the drone is collecting the trajectory of a moving object on the ground. Solve the change pattern of the shooting angle of the drone.

Considering the actual motion characteristics of objects such as cars, it is assumed that the ground targets being tracked are a class of moving bodies with non-integrity constraints. Therefore, the ground-based target model and the small UAV system model based on the reference flight dynamics nonlinear model are established. Using the target tracking algorithm, the motion trajectories of the two groups of objects are generated to solve the shooting angle of the drone.

Task 4: When the drone encounters obstacles such as signal towers, utility poles, houses, etc. during flight, calculate the optimal flight speed, flight altitude and shooting angle of the drone, and provide relevant data simulation experiments.

Therefore, the path is planed based on RRT algorithm, improve the way of parent node selection in the original RRT algorithm, use cost function to select the node with the lowest cost in the extended node domain as the parent node, and recalculate for the two new nodes.

Then, in order to simplify the problem, the path planning obstacles take more regular geometric shapes, such as circles and polygons. Using MATLAB to select a reasonable obstacle avoidance strategy, logically judge each of the above obstacles, that is, the expansion of the random tree can be avoided. Open the obstacle and search for the path from it.

II. Analysis and Assumptions

2.1. Data analysis

2.1.1. Flying height
When using a drone for low-altitude aerial photography, a wide range of captured images are quickly obtained [25-27]. As the aerial photography height increases [28], the model recognition effect shows a downward trend. It has good robustness for keeping shooting recognition in different regions, and can be easily applied to the monitoring and management of various topographic terrains. According to the different height model identification results, the aerial photography height should not be too high. And the aerial photography height is between 10m-120m.

2.1.2. Flight speed
Low-altitude UAV remote sensing is smaller and more flexible than traditional measuring aircraft such as satellites and space shuttles. Therefore, the reference parameter model is the technical parameters of the CW-20 Dapeng UAV, which is a small and medium-sized hybrid electric vertical take-off and landing fixed-wing UAV system with a fuselage length of 1.8m and a wingspan of 3.2m. 2~3kg, wind resistance capacity 7th, battery life 3h, cruising speed is 0-80m/s. Considering that the aerial drone is also divided into military and civilian use, the speed constant in this paper is 40m/s.

2.1.3. Shooting angle
By referring to the reference [29], it can be seen that in the wind resistance, the Kalman filter filter is combined with the gyro value to perform self-adjustment when the drone is tilted and tilted at the maximum angle. Optimize the maximum shooting angle of the aircraft. The MATLAB algorithm is used to calculate the PID value of the UAV in the maximum wind resistance. Combined with the Kalman filter, the ApmWB3.11 flight controller with Kalman filter and gyroscope is designed. The experimental data in the simulator. It shows that the flight controller designed by this combination method is the most stable, and the reaction speed is the fastest, and the stabilization time in the strong wind is longer. Based on this, the shooting angle constant is 75°.

2.2. Symbol Description

Table 1. Symbol Description

Num	Symbol	Description
1	S	Camera acquisition range area
2	θ	shooting angle
3	h	drone flight height
4	DPI	Number of pixels per inch of image length
5	P	The number of frames per second

The symbols involved are shown in Table 1，Unmarked symbols are stated in the paper.

2.3. Fundamental assumptions

(1) Assume that the shape of the drone and the thickness of the fuselage have little effect on the flight results, that is, the influence factors of the drone model are ignored.

(2) Assume that the distribution of pressure during the flight of the drone is uniform, that is, the pressure is negligible.

(3) There are some differences between different types of drones. All theoretical analysis is based on the drone, which ignores the differences between other models.

(4) Assume that the speed of the aircraft is uniform, that is, the speed instability of the drone for reconnaissance missions is not considered.

(5) It is assumed that the weather is normal when the drone is being investigated, that is, the special circumstances affecting the flight such as lightning and storm are not considered.

III. Material and Methods

3.1. Task one：Optimal aerial height model for linear flight

3.1.1. Basic technical parameters

Firstly, the technical parameters of UAV are analyzed from two angles: the drone itself and the picture taken. The technical parameters of the drone itself include the flying height h, the flying speed v and the shooting angle θ. For the specific values and analysis, please refer to the first subsection of Chapter 2 of this paper.

From the perspective of the captured image, the image affected by the drone mainly includes three parameters, the camera acquisition range area S, the pixel number DPI of the image per inch length, and the frame number P of the camera acquisition image per second. This article mainly introduces the above three basic technical parameters.

(1) Camera acquisition range area(S)

The area range S collected during the aerial photography of the drone will vary according to the variation of the flying height h and the shooting angle θ. As shown in the following figure1,the solution will be based on the collective relationship between the three.
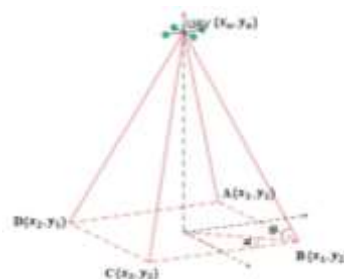

Fig 1: Geometric relationship

As shown in figure1, a Cartesian coordinate system is established by the UAV to create to the ground projection, and the four points on the boundary of the shooting range are recorded as A, B, C, D. Where θ is the shooting angle. α is shown as the angle of the line.

Get the following relation:

$$S = [(x_u + \frac{h}{\tan\theta} \cdot \sin\alpha) - (x_u - \frac{h}{\tan\theta} \cdot \sin\alpha)][(y_u + \frac{h}{\tan\theta} \cdot \sin\alpha) - (y_u - \frac{h}{\tan\theta} \cdot \sin\alpha)] \quad (1)$$

Where S is the camera acquisition range area and h is the drone flight height.

(2) Number of pixels per inch of image length

The second parameter that will be discussed is the number of pixels per inch of the image, or DPI. It is an important measure of the resolution of an image. In general, the larger the DPI value, the clearer the acquired image.

Fig 2: DPI comparison

As shown in figure 2, the pictures displayed by different DPIs have different clarity effects. The picture width pixel is equal to the width of the picture. The DPI is multiplied by the size, and the picture height is the same as the pixel. Therefore, if the image is 1DPI, this means that a 1 by 1 monochrome square is seen per square foot. If it is 100 DPI, it means 100 small squares in the horizontal direction and the vertical direction. There are 10,000 small squares per square foot.

(3)The number of frames per second (*P*)

Frames, short for the number of frames generated, can also be understood as the number of still pictures. Each frame is a still image, and the fast and continuous display of the frame creates an illusion of motion, so a high frame rate results in a smoother, more realistic animation. According to the concept, get the following formula:

$$Fr = p / t \qquad (2)$$

Where *Fr* is Frame rate, *p* is Frames, and *t* is Time. The frame rate is in frames per second fps. In general, 30fps is acceptable, but improving performance to 60fps can significantly improve the sense of interaction and realism, but in general, more than 75fps is generally not easy to notice a significant increase in fluency. If the frame rate exceeds the screen refresh rate, it only wastes the ability to process graphics, because the monitor cannot be updated at such a fast speed that the frame rate exceeding the refresh rate is wasted.

3.1.2. Model establishment

3.1.2.1. Decision variables

(1) Flight altitude - *h*

The flying height of the drone is an important factor. Its size has a direct impact on the range of camera acquisition and the DPI of the acquired image. For example, the flying height increases, the camera acquisition range increases, and the DPI decreases.

(2) Shooting area - *S*

According to the geometric relationship between the shooting area of the drone and the shooting height and shooting angle, the formula as follows:

$$S = (\frac{2h}{\tan \theta} \cdot \sin \alpha)^2 \qquad (3)$$

Where *S* is the Shooting area, *h* is the height at which the drone is located, *θ* is the shooting angle, and *α* is the diagonal angle of the photographic rectangle. Substituting the conventional parameters, the height of the drone is 10m, the shooting angle is 75°, and the unit shooting area is 3.7894m^2.

(3) Pixel accuracy - *P*

Through consulting the technical specifications of the Go Pro HERO8 BLACK camera of the related motion camera and found that the camera can acquire 1600wPX when the shooting distance is 10m and the shooting angle is 75°. That is, there is 1600wPX in one frame of image. The formula is as follows:

$$P = \frac{1600 \times 10^4}{S} (PX/m^2) \qquad (4)$$

Where *P* is Pixel accuracy. The parameters for substituting the area of the drone can be obtained as the number of pixels in the unit area is 422.2304 *w*. Therefore, $P_s = 4222304$ (PX/m^2) is pixel precision.

3.1.2.2. Objective function

According to the requirements of the topic, in the image acquisition process, it is necessary to acquire an image with high definition and a large area of the shooting area as much as possible. Therefore, the objective function is established as:

$$\max \quad w_1 S + w_2 P \qquad (5)$$

In the formula (4), S is the shooting area, P is the pixel precision, and w_1 and w_2 are the weight.

3.1.2.3. Restrictions

(1) Flight altitude

Due to our technology and the presence of high-limit areas in the city, the flight height cannot be too high or too low, so the height of the drone is limited as $h \leq 120$, where h is the flying height of the drone. The height limit area of the city is 50m, and part of the requirement is 120m. Considering the text, the text is set to 120m, which is the maximum flying height of the drone.

(2) Pixel accuracy

Based on the camera height obtained when the camera is above a fixed height, we constrain the pixel precision: $P \geq 80$.

(3) Other variables

According to the requirements of the topic, the flight speed and shooting angle of the drone are constant, so in the solution process, the above two variables are constrained $\theta = 75°, v = 40\mathrm{m/s}$. Where θ is the shooting angle. Take a constant of $75°$, v is the flight speed, take 40m.

In summary, the optimal aerial height model for linear flight for mission one is:

$$obj \quad \max \quad w_1 S + w_2 P$$

$$s.t. \begin{cases} h \leq 120 \\ P \geq 800 \\ \theta = 75° \\ v = 40\,\mathrm{m/s} \end{cases} \qquad (6)$$

3.1.3. Algorithm design and model solving

In this paper, the objective function is treated by the linear weighting method. In theory, we assign the corresponding weight coefficient according to the importance of each target, and then optimize the linear combination. Then, S and P are normalized to remove the dimension, so that the absolute value of the physical system value becomes a relative value relationship, simplifying the calculation. Finally, each of S and P is given a weight of 0.5, that is, both w_1 and w_2 are equal to 0.5.

(1) The core idea of the algorithm

The parameters of the golden section are used to approximate the solution model, where $A_1 = d_2 - 0.618(d_2 - d_1)$ is the left golden point, $A_2 = d_1 + 0.618(d_2 - d_1)$ is the right golden point, and gradually approaches the upper and lower bounds of the height to be sought. When the upper and lower bounds are less than 0.1, the iteration is stopped, and the optimal parameters are obtained.

(2) Algorithm steps

Step1: Let the height $h = A_1$ to be sought, and use the above control model to calculate and calculate the UAV shooting score. If the constraint condition is met, set $flag_1 = 1$, otherwise set it to 0;

Step2: Let the thicknes $h = A_2$ to be obtained, and use the above control model to calculate and calculate the UAV shooting score. If the constraint condition is met, set $flag_2 = 1$, otherwise set it to 0;

Step3: Judging flag. If $flag_1 = 1$, $flag_2 = 1$ or

$flag_1 = 1$, $flag_2 = 0$, the new lower bound is unchanged, and the new upper bound is the original right golden split point; if $flag_1 = 0$，$flag_2 = 1$,the new upper bound is unchanged, and the new lower bound is the original left golden split point; if $flag_1 = 0$，$flag_2 = 0$, stop running;

Step4: Determine whether the difference between the upper and lower bounds is less than 0.1, yes, stop running, no, continue with Step5;

Step5: Find the new upper and lower bounds, and the left and right golden points, repeat Step1-Step4.

Using MATLAB to solve the problem, allowing the drone to take aerial photography in a straight-line flight mode.
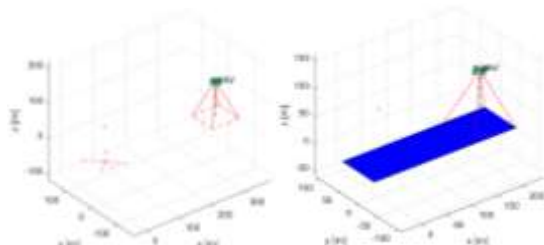
Fig 3: Aerial photography

As shown in figure 3, a visual output of the UAV shooting process, giving the UAV a constant flight speed and shooting angle (v = 60 m/s, θ=75°), and calculating the aerial drone. Shooting at different flight altitudes, solving the model yields:
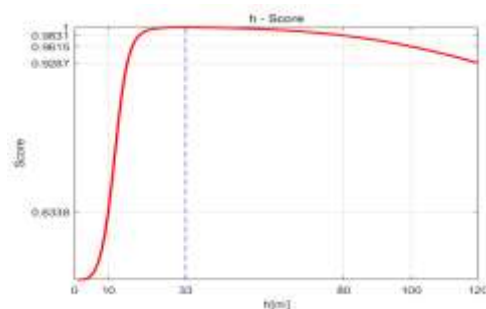

Fig 4. Model result

As shown in figure 4, this paper solves the UAV shooting of the drone between 0 and 120m. It can be seen from the figure that at a flying height of 33m, the best picture can be taken, including the good definition of the image, as well as the appropriate shooting range.

3.2. Task two: UAV shooting angle optimization model

3.2.1. Decision variable correlation analysis

(1)Shooting area & shooting angle

Considering the geometric relationship between the shooting angle (θ) and the camera acquisition range area (S), a rectangular coordinate system is established for UAV shooting system. As shown in Figure5, a rectangular coordinate system is established by UAV projection to the ground, and the four points on the boundary of the shooting range are recorded as A, B, C, D. Where θ is the shooting angle. α is shown as the angle of the line. Get the following relationship:

$$S = [(x_u + \frac{h}{\tan\theta} \cdot \sin\alpha) - (x_u - \frac{h}{\tan\theta} \cdot \sin\alpha)][(y_u + \frac{h}{\tan\theta} \cdot \sin\alpha) - (y_u - \frac{h}{\tan\theta} \cdot \sin\alpha)] \quad (6)$$

Where, S is the camera acquisition range area, h is the drone flight height, and θ is the shooting angle. The formula is simplified and the relationship between the two parameters is analyzed:
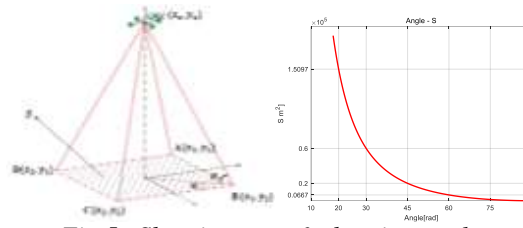
Fig 5. Shooting area & shooting angle

As shown in figure 5, there is a negative correlation between the shooting angle and the camera's acquisition range. When θ is taken as 20°, 30°and 45 respectively, the ratio of the area of the unmanned aerial vehicle can be 1.5097m², 0.6m², 0.2m².

(2) Shooting area & pixel accuracy

Considering the geometric relationship between pixel accuracy (P) and camera acquisition range area (S), we solve the numerical relationship between the shooting area and pixel accuracy of the drone. According to the technical specifications of the Go Pro HERO8 BLACK camera of the motion camera, it is known that the camera can acquire 1600wPX when the shooting distance is 10m and the shooting angle is 75°. That is, there is 1600w PX in one frame of image. Substitute the corresponding constant value to get:

$$S = (\frac{2h}{\tan\theta} \cdot \sin\alpha)^2 = (\frac{2\times10}{\tan75°} \cdot \sin45°) = 3.7894 \text{ m}^2 \quad (7)$$

$$P = \frac{16000\times10^4}{S} \text{(PX/ m}^2) \quad (8)$$

In the formula, P is the pixel precision, S is the camera acquisition range area, h is the drone flight height, and θ is the shooting angle. Therefore, it can be seen that the number of pixels in the unit area is 422.2304 w, which is substituted into the solution, and the pixel precision is 4222304 PX/m².

(3)Flying height & shooting area

Considering the geometric relationship between flight height (h) and camera acquisition range area (S), a rectangular coordinate system is established for UAV shooting system. As shown below:
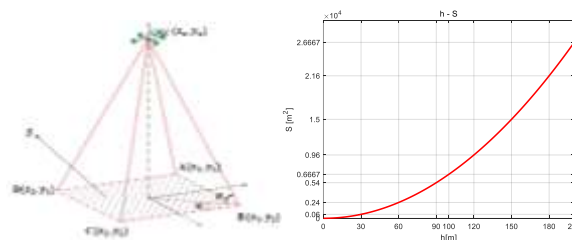

Fig 6: Flying height & shooting area

As shown in figure 6, this paper solves the relationship between the two based on the established Cartesian coordinate system. It is founded that the range of camera acquisition range of drones increased with height, and the two were in a positive relationship. Among them, when the flying height of the drone is 60m, 90m and 120m respectively, the camera collection range is 0.24m², 0.54m² and 0.96m² respectively.

(4) Shooting angle & pixel accuracy

The above analysis of the relationship between the shooting angle of the drone and the camera acquisition range area and the camera acquisition range area and pixel accuracy. Therefore, under the premise of two proportional

$$S = (x_u + \frac{h}{\tan\theta} \cdot \sin\alpha - x_u + \frac{h}{\tan\theta} \cdot \sin\alpha)(y_u + \frac{h}{\tan\theta} \cdot \sin\alpha - y_u + \frac{h}{\tan\theta} \cdot \sin\alpha)$$

relationships, the correlation between the shooting angle and the pixel accuracy of the UAV is solved in conjunction to further analyze.

$$(9)$$

$$S = (\frac{2h}{\sqrt{3}} \cdot \frac{\sqrt{2}}{2})^2 = \frac{4h^2}{3} \cdot \frac{2}{4} = \frac{2h^2}{3} \qquad (10)$$

In the formula, P is the pixel precision, S is the camera acquisition range area, h is the drone flight height, and θ is the shooting angle. A negative correlation between the shooting angle and the pixel precision is obtained by substituting $\alpha=40^o$ and $\theta=60^o$.

3.2.2. Model establishment

3.2.2.1. Decision variables
Same as the first problem, the decision variables in this paper are still Flight altitude (h), Shooting area (S) and Pixel accuracy (P). Since the above decision variables have been described in detail in Question 1, there is no longer a lot of introduction in this chapter.

3.2.2.2. Objective function
According to the requirements of the topic, in the image acquisition process, the drone needs to perform more accurate image acquisition under actual ground conditions, so linearly weight the shooting area and pixel precision to establish the objective function in formula (5).

3.2.2.3 Restrictions
(1)Flight altitude
Due to our technology and the presence of high-limit areas in the city, the flight height cannot be too high or too low, it is limited $h \le 120$.Where h is the flying height of the drone. The height limit area of the city is 50m, and part of the requirement is 120m. Considering the text, the text is set to 120m, which is the maximum flying height of the drone.

(2) Pixel accuracy
Based on the camera height obtained when the camera is above a fixed height, the pixel precisionis constrained here: $P \ge 800$.

(3)Other variables
According to the requirements of the topic, the flight speed of the drone is constant, so in the solution process, the above two variables are constrained v=40m/s.

(4) Constant value
The two variables of the objective function are given here, which are the shooting area and pixel precision of the drone:

$$\begin{cases} P = \dfrac{1600 \times 10^4}{S} \\ S = (\dfrac{2h}{\tan\theta} \cdot \sin\alpha)^2 \end{cases} \qquad (11)$$

In the formula (11), P is the pixel precision, S is the camera acquisition range area, h is the drone flight height, and θ is the shooting angle.

In summary, the UAV shooting angle optimization model established for Task 2 is:

$$obj \quad max \quad w_1 S + w_2 P$$

$$s.t. \begin{cases} h \leq 120 \\ P \geq 800 \\ S = (\dfrac{2h}{\tan\theta} \cdot \sin\alpha)^2 \\ P = \dfrac{1600 \times 10^4}{S} \end{cases} \quad (12)$$

3.2.3. Algorithm design and model solving

According to the requirements of the topic, the drone needs to perform more accurate image acquisition under actual ground conditions. Therefore, the two variables of camera acquisition range area and image precision are given weights of 0.4 and 0.6, respectively, ie w_1=0.4, w_2=0.6. The algorithm core and the center step are the same as task 1, but the angle of the initial value needs to be changed.

UsIing MATLAB to solve the best shooting angle under the optimal flight height that the UAV has solved in Task 1. The specific results and the UAV visualization results are as follows:
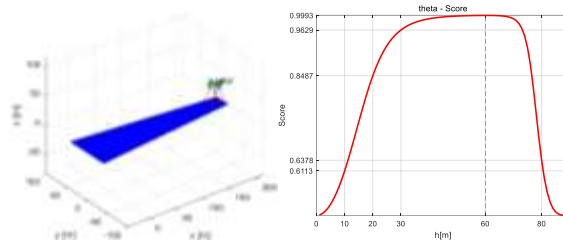
Fig 7: Best shooting angle at different heights

As shown in figure 7, when the speed is a constant value of 40 m/s and the height is 33 m, the optimum shooting angle is 59.9961 degrees. The height of 33m is the solution result of task one. When the flight speed is constant, the flight field and the shooting angle are related to the field of the score as shown below:
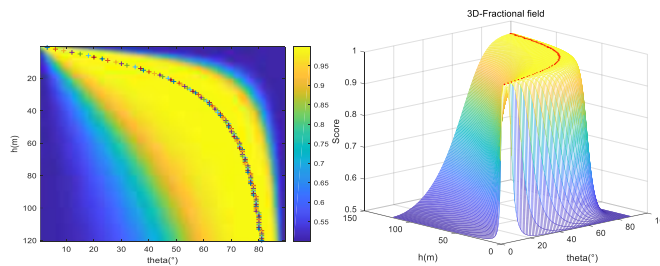

Fig 8. Fractional field

The above figure 8 is the two-dimensional fractional field on the field of the fractional field. The most advantageous of the visualization in the two-dimensional fractional field is the plus sign. Finally, the fixed height is determined. At a constant speed, the optimum shooting angle range is [56.2248°-77.4972°].

3.3. Task three: UAV shooting angle change mode

3.3.1. Ground target model

When the drone is collecting the trajectory of a moving object on the ground, considering the actual motion characteristics of the object such as a car, we assume that the ground target being tracked is a type of moving body with non-integrity constraints. Therefore, a kinematic model of the target is:

$$\begin{cases} \dot{x}_t = v_t \cdot \cos\psi_t \\ \dot{y}_t = v_t \cdot \sin\psi_t \\ \dot{v}_t = w_t \end{cases} \qquad (13)$$

Where (x_t, y_y) represents the position of the target in plane $X^S Y^S$. v_t and ψ_t represent the speed and direction of the target motion, respectively. The target speed is divided into discrete and continuous states.

3.3.2. Small UAV system model

For the flight dynamics nonlinear model of the drone, considering that the UAV is a multi-body system, the motion coupling, the inertia coupling, the structural coupling and the pneumatic coupling of the rotor, the body, the lifting surface, etc. Constant and nonlinear characteristics bring many difficulties to UAV flight dynamics modeling. The physical model of each moving part and its mathematical expression must be fully considered when establishing the mathematical equation of UAV motion. Therefore, a nonlinear model of flight dynamicsis established as follows:

$$\dot{x} = f(x, u, t) \qquad (14)$$

In the formula (14), $x \in R^9$ represents the state variable of the small UAV, including the three-dimensional position $[x_1, y_1, z_1]^T$ and the attitude angle $[\phi, \theta, \psi]^T$ in the world coordinate system, and the three-dimensional linear velocity $[u, v, w]^T$ in the body coordinate system.

Next, the specific expression of the translational model will be given to model the UAV dynamics. According to the relationship between the world coordinate system and the body coordinate system, the displacement equation of the small UAV motion can be obtained as:

$$\begin{bmatrix} x_1 \\ y_1 \\ z_1 \end{bmatrix} = {}_b^\varsigma R \cdot \begin{bmatrix} u \\ v \\ w \end{bmatrix} \qquad (15)$$

In formula (15), the matrix ${}_b^\varsigma R$ represents the rotation matrix of the coordinate system $\sum_b$ to the other coordinate system $\sum_\varsigma$, and the attitude of the drone represented by the Euler angle is determined:

$$ {}_b^\varsigma R = \begin{bmatrix} c\theta c\psi & s\theta s\varphi c\psi - c\varphi s\psi & s\theta c\varphi c\psi + s\varphi s\psi \\ c\theta s\psi & s\theta s\varphi s\psi + c\varphi c\psi & s\theta c\varphi s\psi - s\varphi c\psi \\ -s\theta & c\theta s\psi & c\theta c\varphi \end{bmatrix} \qquad (16)$$

In formula (16), s and c represent $\sin(\cdot)$ and $\cos(\cdot)$, respectively. Considering the small UAV body, all the components except the main rotor and the balance wing as the ideal rigid body, the dynamic equation of the translational motion of the UAV can be derived by using the Newton-Eulerian equation of the rigid body motion.

$$\begin{bmatrix} \dot{u} \\ \dot{v} \\ \dot{w} \end{bmatrix} = S(p, q, r) \cdot \begin{bmatrix} u \\ v \\ w \end{bmatrix} + \frac{1}{m} \begin{bmatrix} G_x + F_x \\ G_y + F_y \\ G_z + F_z \end{bmatrix} \qquad (17)$$

Where $S(p, q, r) \in R^{3\times3}$ represents the antisymmetric matrix, given by (18):

$$S(p, q, r) = \begin{bmatrix} 0 & r & -q \\ r & 0 & p \\ q & -p & 0 \end{bmatrix} \qquad (18)$$

In formula (17), $m \in R$ represents the mass of the UAV, and the force of the UAV in each axial direction is com-

posed of two parts, where $[G_x, G_y, G_z]^T$ represents the component of the UAV's gravity in the three axes of the body coordinate system, expressed as:

$$\begin{cases} G_x = -mg\sin\theta \\ G_y = mg\cos\theta\sin\varphi \\ G_z = mg\cos\theta\cos\varphi \end{cases} \quad (19)$$

$[F_x, F_y, F_z]^T$ represent the component of the three axes of aerodynamics in the body coordinate system. The aerodynamic force of each axis is the resultant force of the main rotor and the fuselage of each component of the UAV.

3.3.3. Algorithm design and model solving

In Task 3, the algorithm steps involved in the good small UAV system model based on the ground target model are:

Step1: Initialize the v, theta, h of the drone and the Vm of the target point;

Step2: Time lapse, computer simulation;

Step3: Get the real-time speed Vm of the target point through the current time and calculate the target point position at the next moment;

Step4: Calculate the current shooting range of the drone, and judge whether the target point position is within the capture range. If yes, return to Step2. If no, recursively adjust the shooting angle according to the target point position;

Step5: Whether to reach the final moment, if yes, the algorithm ends, if not return to Step2.

(1) Discrete motion

Using MATLAB to solve the problem. When determining the relationship between the camera's acquisition range and the object, we first generate two-dimensional trajectories of two moving objects:
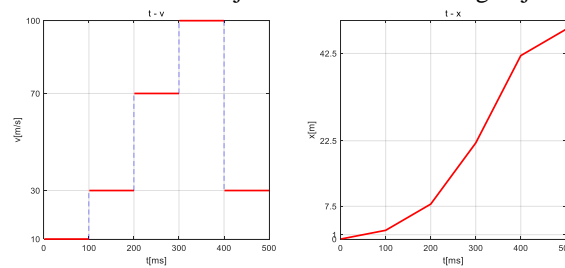

Fig 9. Speed and displacement changes

The above figure 9 shows the change of the speed and displacement of the drone with respect to time. It can be seen from the figure that the movement of the first group of objects is a discrete case, and the speed change is abrupt change. Using MATLAB to display the visual results, taking the case of drones in 1s, 3s, and 5s as an example:
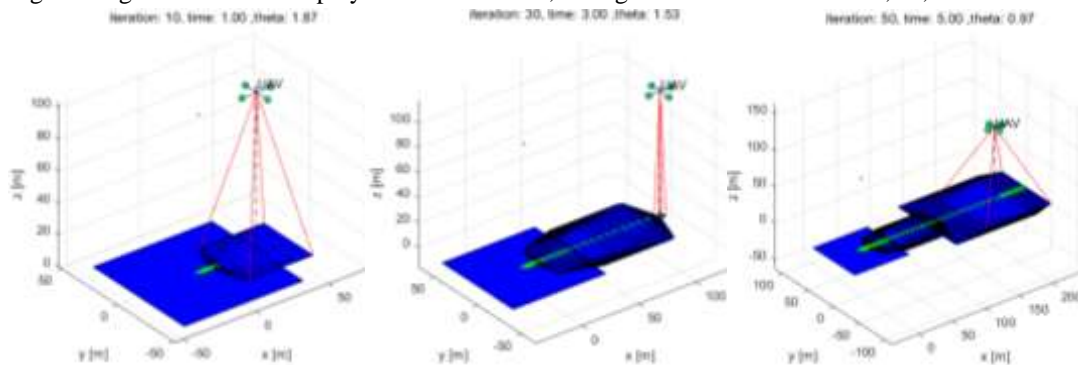

Fig10: Discrete motion

The above figure 10 shows the trajectory of a moving object on the ground being collected by the drone. It is assumed that the flying height of the drone is fixed and the flying speed is constant. The result of the model solution is:
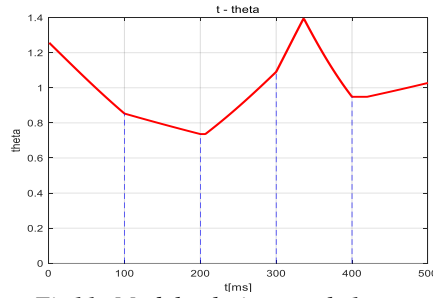

Fig11: Model solution result 1

As shown in figure 11 , the shooting angle θ varies with time, and its range is [0.7362, 1.3940], that is, [42.18^{o}, 79.87^{o}].

(2) Continuous motion

Next, the continuity of the moving object between the camera's acquisition range and the object will be determined.
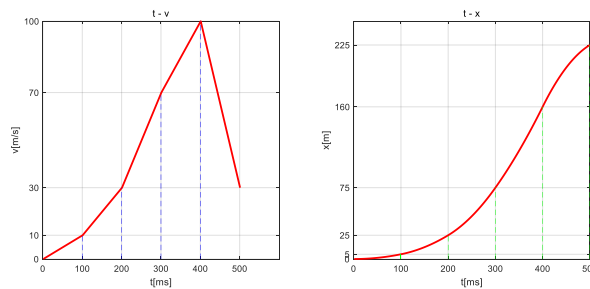

Fig 12: Speed and displacement changes

The two-dimensional trajectory is shown below:

The above figure 12 shows the change of the speed and displacement of the drone with respect to time. It can be seen from the figure that the second group of objects is a continuous motion, which has a continuous constant acceleration in different time periods. Using MATLAB to visualize the results, as well as the case of drones in 1s, 3s, and 5s:
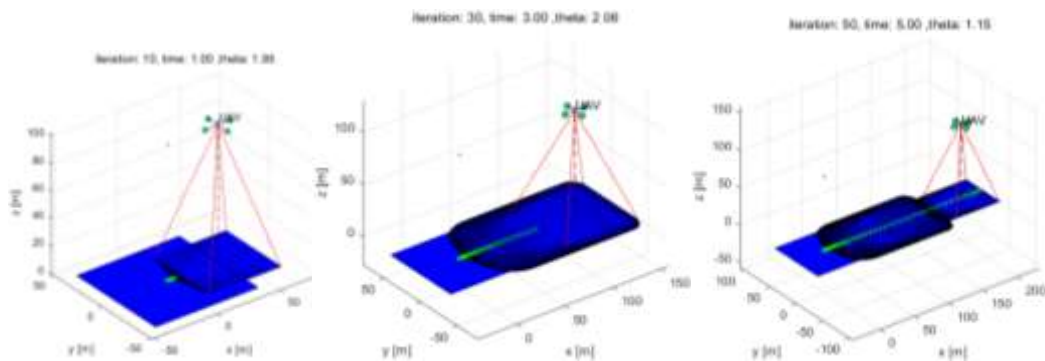

Fig 13. Continuous motion

The above figure 13 shows the trajectory of a moving object on the ground being collected by the drone. It is assumed that the flying height of the drone is fixed and the flying speed is constant. The result of the model solution is:
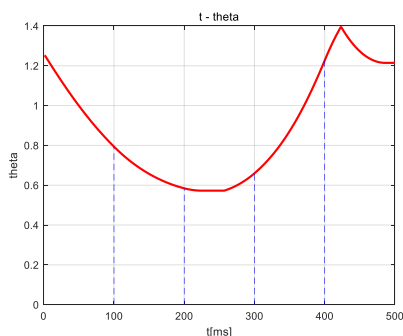
Fig14. Model solution result 2

As shown in figure 14, the shooting angle θ varies with time, and its range is [0.5726, 1.3944] or [32.81°, 79.89°].

3.4. Task four：Obstacle data simulation

3.4.1. RRT-based path planning
The RRT algorithm is a relatively efficient algorithm with good processing results. It has great advantages for dealing with path planning problems with non-integrity constraints. However, the RRT algorithm can only obtain path feasible solutions, not optimal solutions. . Therefore, in order to solve the optimization problem, the RRT* algorithm is proposed.

(1) Reselect the parent node

In the original RRT algorithm, the algorithm improves the way of parent node selection. The cost function is used to select the node with the lowest cost in the extended node domain as the parent node. At the same time, the nodes on the existing tree are reconnected after each iteration. Thereby ensuring the computational complexity and the progressive optimal solution.
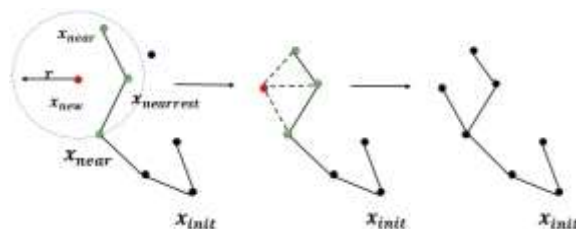

Fig 15: Reselect the parent node process

As shown in figure 15, look for "near neighbors" within a defined radius around the newly generated node as an alternative to replacing the parent node. The path cost of the "near neighbor" node to the starting point is calculated in turn plus the path cost to each "neighbor". The process of reselecting the parent node of RRT* is:

Step1: Take X_{new} as the center and r as the radius (for the predetermined radius), call the near() function to select nearby nodes, and fall in this area are all X_{near} subsets;

Step 2: Set X_{new} to the minimum value, and the path cost from the initial point to $X_{nearrest}$ and X_{min} to X_{new} is set to the minimum path cost C_{min}；

Step3: Next, iterate through all the points in the nearby node set. If the path of the new connection costs less than C_{min}, then the new X_{near} is taken as X_{min}, and the minimum path cost is the sum of the node to the initial node and the node to X_{new}. Finally add the connected edges to this tree.

(2) Rewiring random tree process

The convergence time of the RRT* algorithm is a prominent research problem. At the same time, the difference between the RRT* algorithm and the RRT algorithm lies in the two recalculation processes for the new node, which are the process of re-selecting the parent node and the rewiring random tree. Process. The former has been introduced above, the process of rewiring the random tree is analyzed:
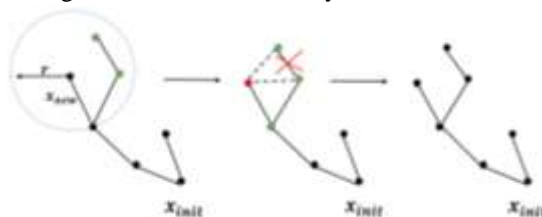

Fig 16. Rewiring random tree process

As shown in figure 16, the significance of the rewiring process is that the path cost of some nodes is reduced by rewiring each time a new node is generated. If viewed from a holistic perspective, not every rewiring node will appear in the resulting path, but in the process of generating a random tree, each rewiring will create as much opportunity as possible for the final path cost reduction. The specific process is:

Step1: First traverse the remaining X_{near} in the nearby node set;

Step2: If the path cost of a certain X_{near} to X_{new} plus the path from the initial point to X_{new} is less than this point, and the collision detection is qualified. Then tentatively A as the parent node;

Step3: Delete all other X_{near} connected to the parent node and add the path to re-weld.

3.4.2. Obstacle avoidance strategy selection and algorithm design

In order to simplify the problem, the obstacles of the path planning take more regular geometric shapes, such as circles and polygons. For circular obstacles, the determination of circular boundaries is a nonlinear problem, and the circle is usually linearized (converted into polygons). It is only necessary to judge whether the horizontal and vertical coordinates are within the circle. If X_{new} is located in the circumscribed square of the circular obstacle, it is regarded as a collision. The collision conditions are:

$$x_0 - r - inf < x_{new,x} < x_0 + r + inf$$
$$y_0 - r - inf < x_{new,y} < y_0 + r + inf \quad (20)$$

In the formula (20), the circular obstacle has a center coordinate of (x_0, y_0) and a radius of *r*. Consider the target moving size, puffing the obstacle, and expanding the size inf.

In the simulation environment, rectangular obstacles are mainly selected. Therefore, the specific collision mechanism is that in the process of expanding the random tree, the edge connected by X_{near} to X_{new} cannot intersect with any side of the rectangular obstacle, that is, the problem of collision detection of the rectangular obstacle is converted into the intersection of the straight line and the rectangle. Therefore, it can be concluded that:

First determine if they are on one side of a side of the rectangle. If it is on the same side of any side of the rectangle, then no subsequent judgment is required, and the line must not intersect the rectangle. There is no case where two points are inside the rectangle, because X_{new} is generated by X_{near}, and X_{near} must be outside the rectangle. If it is located on both sides of a certain side, the second step is judged. The pseudo code is judged as follows Table 2:

Table 2 Algorithm Design of Obstacle Avoidance Strategy

$Algorithm \quad GENERATE\_RRT(x_{init}, K, \Delta t)$

$T.init(x_{init});$

$for\ k = 1\ to\ K\ do$

$if\ (\|x_{new} - x_{goal}\| < d)$

$\quad break;$

$x_{rand} \leftarrow RANDOM\_STATE();$

$x_{near} \leftarrow NEAREST\_NEIGHBOR(x_{rand}, T);$

$u \leftarrow Select\_input(x_{rand}, x_{near});$

$x_{new} \leftarrow NEW\_STATE(x_{near}, u, \Delta t);$

$judge(x_{new});$

$if\ (judge(x_{new}) == false\ and\ colisionfree() == false)$

$\quad continue;$

$T.add\_vertex(x_{new});$

$T.add\_edge(x_{near}, x_{new}, u);$

$return\ T$

To continue to judge the different sides of either side of the rectangle, consider the following two situations:

(1) X_{new} is inside the rectangle, and the line must intersect the rectangle.

(2) Both points are outside the rectangle. In this case, there is no guarantee that the two-point line does not intersect the rectangle. The two points are outside the rectangle and are on either side of the upper side of the rectangle, but the two-point line intersects the rectangle. In this case, the collision avoidance calculation is performed using the properties of the straight line and the rectangle.

By performing the above logical judgment for each obstacle as described above, the expansion of the random tree can be avoided and the path can be searched for.

3.4.3. Model solving

This is set a total of 9 obstacles within 5 seconds, that is, the drone flies over 200m, generating 1 skyscraper, 2 signal towers, 3 telephone poles, and 3 residential buildings. Use RRT* to make obstacle avoidance strategy choices. Take the results of signal towers, skyscrapers and residential buildings as an example. The results are as follows:

Fig 17. Obstacle Avoidance Strategy

Assuming that the main obstacles are signal towers, skyscrapers, and residential buildings, the trajectory map of the UAV path is shown in the above figure 17, and the residential building is selected to be about 30 stories high. Their heights are 52 m / 72 m, 100 m and 90 m respectively.
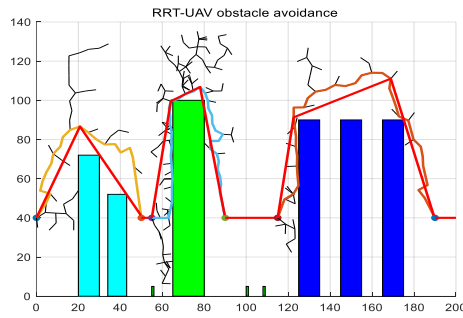
Fig 18. Task 3 obstacle avoidance results

As shown in figure 18, the red line is the optimal path planning for the UAV. In this case, we first optimize the obstacle avoidance route for each part, and then smooth the processing to obtain the global optimal route. When 9 obstacles appear at the same time, the flying height of the drone in the urban area needs to be controlled at about 40m. After lifting off the obstacle, it is necessary to quickly return to a height of 40 m.

IV. Test the Models and Sensitivity Analysis

4.1. Test the Models

It is observed that S is a nonlinear relationship with respect to h, and when h reaches a certain height, the imaging area S is more and more affected by h. In the actual situation, h should be linear with the length of the shooting area, and the shooting area programming and shooting area are nonlinear, so h and the shooting area are also non-linear. In line with the actual situation, the model is reasonable.
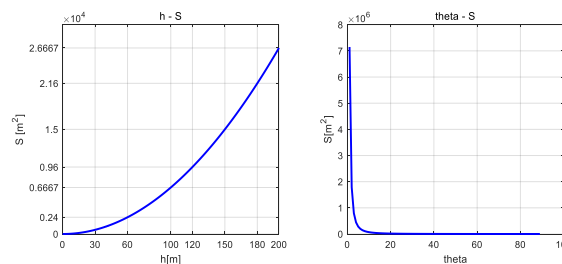

Fig 19. Test the Models

As shown in figure 19, the *S* is a nonlinear relationship with theta, and when theta is extremely small, the shooting area is infinite. In reality, when theta angle is extremely small, the camera light will cover the entire area before its decay is complete. When the theta is between 30° and 70°, the area of the S area does not change much. In line with the actual situation, the model is reasonable.
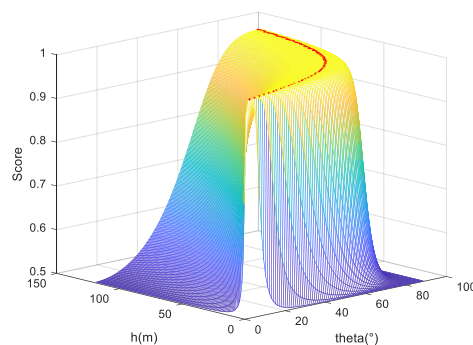
4.2. Sensitivity Analysis

Fig 20: Sensitivity Analysis

As shown in figure 20, the optimal score point is the red dot at the corresponding flight height and shooting angle. The vast majority of the most advantageous height range is [30m, 100m], and First question get the optimal height 33 m in its range, the model has good robustness. Most of the best points are in the range of [40°, 80°]; the results obtained from the second and the third questions [56.2248°,77.4972°], [32.81°, 79.89°] are in good agreement and the model is stable. And in the case of a fixed height, theta changes from 0° to 30°, and the variation is huge.

V. Conclusion

For the first question, the geometric relationship between the flying height and the camera's acquisition range area is analyzed. Then, setting a pixel accuracy score index as the criterion. The sum of the weighted capture area and the pixel accuracy score is taken as the objective function, the flight height does not exceed the height limit area, and the unit pixel point is greater than 800 as the constraint condition. An optimization model for the accuracy of drone shooting was established. Using computer simulation to solve the accuracy method step by step. Getting the height range of the drone is [25m, 100m], the optimal aerial height is 33m when the $\theta=60°$.

For the second question, based on the first question, the numerical relationship between the shooting angle and the camera acquisition range area is analyzed. The sum of the captured area and the pixel accuracy score after updating the weight is the objective function, the shooting angle is the decision variable, and the UAV shooting accuracy score optimization model is used. And use the golden section algorithm to solve. It is determined that when the flying speed of the drone is 40m/s and the flying height is 33m, the optimal range of the shooting angle of the drone is[56.2248°,77.4972°].

For the third question, based on the knowledge of robotics, a small UAV system model and a ground target model are established. Motion trajectories of discrete and continuous states of the object are generated. And the recursive target tracking algorithm is used to continuously adjust the UAV shooting angle to ensure that the target is within its shooting area. Finally, the corresponding values of the two shooting angles with respect to time are obtained. The range of angle changes is respectively [42.18°, 79.87°] and [32.81°, 79.89°].

For the fourth question, it is generated 1 skyscraper, 2 signal towers, 3 telephone poles, 3 30-story residential buildings, a total of 9 obstacles. We improved the traditional fast search random tree model parent node selection method. The cost function is used to select the node with the lowest cost in the extended node domain as the parent node, and the two new nodes are recalculated. And determined the obstacle avoidance logic judgment strategy. Finally, the obstacle avoidance strategy of the drone was obtained.

Finally, the rationality of the model is verified. Through computer simulation, it is determine that the three-dimensional field of flight speed constant, flying height and shooting angle with respect to the score, which proves Model stability and robustness.

This paper has conducted in-depth research on the ground photography technology of drones, and the research focuses on the following three aspects:

(1)The relationship between the flying height h shooting angle and the flying speed with respect to the pixel accuracy score is established.

(2)Research on the real-time shooting angle adjustment strategy of the UAV for moving targets.

(3)Research on RRT algorithm of UAV random tree obstacle avoidance strategy.

With rigorous logic, the mechanism analysis is relatively thorough. And using the golden section method, recursive and other optimization algorithms, the results are obtained accurately and efficiently. Through the analysis and

research of the results, it is concluded that the mathematical model of the whole article is reasonable, stable and robust. We visualize the drones, the environment, obstacles, and shooting areas visually.

However, since the moving speed of the tracked target is randomly generated, it often does not conform to the moving characteristics of objects in real life; the relative position of the obstacles generated may not conform to the real-life architectural layout; therefore, it does not have industrial value, but has very strong academic research value.

References

[1] Tripolitsiotis, Prokas.Kyritsis;Dollas;Papaefstathiou;Partsinevelos,Dronesourcing: a modular, expandable multi-sensor UAV platform for combined, real-time environmental monitoring,International Journal of Remote Sensing38(8-10)(2017), 2757-2770.

[2] K. Zhao, T. T. He, S. Wu; S. L. Wang, B. Dai, Q. F. Yang, Y. T. Lei, Application research of image recognition technology based on CNN in image location of environmental monitoring UAV, EURASIP Journal on Image and Video Processing2018, (1)(2018),1-11.

[3] Z.W. Li; Y. L; Y. Shi; Z.G. Wang; W.X. Qiao; Y.C. Liu,A Dyna-Q-Based Solution for UAV Networks Against Smart Jamming Attacks,Symmetry11(5)(2019),617.

[4] M. B. Bejiga, A. Zeggada, A. Nouffidj, F. Melgani, A Convolutional Neural Network Approach for Assisting Avalanche Search and Rescue Operations with UAV Imagery,Remote Sensing9(2)(2017).

[5] L. Zheng, J. B. Hu, S. K. Xu, Marine Search and Rescue of UAV in Long-Distance Security Modeling Simulation,Polish Maritime Research24(s1)(2017), 192-199.

[6] M. Półka, S. Ptak; Ł. Kuziora, The Use of UAV's for Search and Rescue Operations,Procedia Engineering192(2017),748-752.

[7] G.Nugroho, A. A. R. Jani, R. R. T. Sadewo, Manufacturing Process and Flight Testing of an UAV with Composite Material,Applied Mechanics and Materials4225(2016),311-318.

[8] V.S. Juan, M. Santos, Intelligent UAV Map Generation and Discrete Path Planning for Search and Rescue Operations, Complexity2018(2018), 6879419.

[9] M. Rodzewicz, D. Glowacki, Investigations into Load Spectra of UAVS Aircraft, Fatigue of Aircraft Structures 5(2013), 40-52.

[10] C. Goerzen, Z. Kong, B. Mettler, A Survey of Motion Planning Algorithms from the Perspective of Autonomous UAV Guidance,Journal of Intelligent and Robotic Systems57(1-4)(2010),65-100.

[11] L. Babel, Three-dimensional Route Planning for Unmanned Aerial Vehicles in a Risk Environment, Journal of Intelligent & Robotic Systems 71(2) (2013),255-269.

[12] X. Niu, X. D. Yuan, Y.W. Zhou; H. H. Fan, UAV Track Planning Based on Evolution Algorithm in Embedded System,Microprocessors and Microsystems75(2020),15-27.

[13] F. Ropero, P. Muñoz, TERRA: A path planning algorithm for cooperative UGV–UAV exploration, Engineering Applications of Artificial IntelligenceVolume 78(2019), 260-272.

[14] Y. Huang; J.G. Chen; H.L. Wang; G.F. Su, A method of 3D path planning for solar-powered UAV with fixed target and solar tracking,Aerospace Science and Technology92(2019), 831-838.

[15] P.S. Krishnan; K. Manimala, Implementation of optimized dynamic trajectory modification algorithm to avoid obstacles for secure navigation of UAV,Applied Soft Computing90(2020),123-234.

[16] I. Karakostas;I. Mademlis;N. Nikolaidis,Shot type constraints in UAV cinematography for autonomous target tracking,Information Sciences506(2020),273-294.

[17] Sara, Pérez-Carabaza, Jürgen Scherer; Bernhard Rinner;José A. López-Orozco; EvaBesada-Portas, UAV trajectory optimization for Minimum Time Search with communication constraints and collision avoidance,Engineering Applications of Artificial Intelligence85(2019),357-371.

[18] A. Albert; L. Imsland, Combined Optimal Control and Combinatorial Optimization for Searching and Tracking Using an Unmanned Aerial Vehicle,Journal of Intelligent & Robotic Systems95(2)(2019),691-706.

[19] Massimiliano, Iacono, Antonio Sgorbissa, Path following and obstacle avoidance for an autonomous UAV using a depth camera, Robotics and Autonomous Systems 106 (2018), 38-46.

[20] P. Sun, A. Boukerche, Performance modeling and analysis of a UAV path planning and target detection in a UAV-based wireless sensor network, Computer Networks146(2018), 217-231.

[21] H. Huang, Research on the measurement of key target point spacing based on aerial image of UAV, Computer Measurement & Control 27(07)(2019),11-14+31.

[22] X. L. Zhou, The Application of UAV in TV Camera, Journal of Journalism Research 7(17) (2016),338.

[23] Y. Ji, Z.Y. Q, B.J. W, Application of Small Unmanned Aerial Vehicle Remote Sensing Platform in Photogrammetry, Surveying and Mapping Technology and Equipment (1) (2008), 46-48.

[24] H. Cheng, J. Cao, Z. Chen, Based on unmanned aerial vision without control point dual image stereo positioning and its accuracy analysis, Electronic Design Engineering(11)(2016), 186-188,193.

[25] Z. H. Wang, P. F. Zheng, X. F. Yan, T. Li, G. T. Fu, X. Q. Guo, N. Wei, A Matching Method for Aerial Images of UAVs, Cable TV11(2017),23-25.

[26] Y. S. Li, J. H. Yan, W. X. Xie, L.Q. LI,A new method for rapid stitching of aerial photography sequences of drones, Chinese Journal of Electronics40(5)(2012),935-940.

[27] Y.W. Liu, X. M. Li, Overview of target detection and tracking methods in aerial video of drones, Flying missiles 9 (2016),53-56,70.

[28] X. Z. Wei, R. Ma; J. Zhang, Research on the factors affecting the flight and shooting stability of UAVs, Science Chinese0 (8X) (2017), 32-35.

[29] Z.W. Lin, Q. L. Ding, W. H. Tu, Vegetation type identification based on multi-dimensional Hog and aerial image of drones, Journal of Forest and Environment38(4)(2018),444-450.